CrystEngComm

Accepted Manuscript

ROYAL SOCIETY OF CHEMISTRY

www.rsc.org/crystengcomm

To achieve high-quality $In_{0.3}Ga_{0.7}As$ films on GaAs substrates by low-temperature molecular beam epitaxy

Fangliang Gao[a], Lei Wen[a], Jingling Li[a], Yunfang Guan[a], Shuguang Zhang[*ab], Guoqiang Li[*ab]

[a]*State Key Laboratory of Luminescent Materials and Devices, South China University of Technology, Guangzhou, 510641, China*
[b]*Department of Electronic Materials, School of Materials Science and Engineering, South China University of Technology, Guangzhou 510641, China*

Abstract: The effects of the thickness of the large-mismatched amorphous $In_{0.6}Ga_{0.4}As$ buffer layer on the $In_{0.3}Ga_{0.7}As$ epi-films grown on the GaAs substrate have been systematically investigated. The $In_{0.3}Ga_{0.7}As$ films with the $In_{0.6}Ga_{0.4}As$ buffer layer of 0, 1, 2, 4 nm are grown using the low temperature molecular beam epitaxy (LT-MBE) and are characterized by X-ray diffraction (XRD) and transmission electron microscopy (TEM). It is found that the relaxation degree and crystallinity of the as-grown $In_{0.3}Ga_{0.7}As$ films are strongly affected by thickness of the amorphous $In_{0.6}Ga_{0.4}As$ buffer layer. The thinner $In_{0.6}Ga_{0.4}As$ buffer is not enough to efficiently release the misfit strain between the $In_{0.3}Ga_{0.7}As$ epilayer and the GaAs substrate, while the thicker $In_{0.6}Ga_{0.4}As$ buffer layer is unfavorable to trap the dislocations from extending into the $In_{0.3}Ga_{0.7}As$ epi-films. We have demonstrated that the amorphous $In_{0.6}Ga_{0.4}As$ buffer layer with a thickness of 2 nm can advantageously prevent the threading and misfit dislocations from propagating into the subsequent $In_{0.3}Ga_{0.7}As$ epilayer and increase the relaxation degree of the as-grown $In_{0.3}Ga_{0.7}As$, ultimately leading to a high-quality $In_{0.3}Ga_{0.7}As$ film. Our novel buffer layer technology has triggered a simple but effective approach to grown the high-crystallinity $In_{0.3}Ga_{0.7}As$ epitaxial film and is favorable to fabricate the GaAs-based high efficiency four-junction solar cells.

1. Introductions

In recent years, GaAs-based multi-junction solar cells with the structure of GaInP/GaAs/Ge (band-gap energy 1.84/1.4/0.67 eV) have attracted much interest due to their high efficiency. The conversion efficiency has been higher than 40 % using the above-mentioned conventional triple-junction solar cells structure.[1, 2] From the previous studies, the design principle of the GaInP/GaAs/Ge tandem solar cells structure was to choose the lattice-matched materials in order to achieve high-crystallinity epitaxial films. However, the Ge bottom cell has an approximately two times higher photocurrent density than the middle and top sub-cells, leading to a

* *Authors to whom correspondence should be addressed.*
Emails: mssgzhang@scut.edu.cn; msgli@scut.edu.cn.

large photocurrent mismatch and seriously limited conversion efficiency of the solar cells. Therefore, in order to further improve the conversion efficiency of photovoltaic cells, one of the effective techniques is to insert a sub-cell between the Ge and InGaAs sub-cells to achieve the preferable bandgap matching. Thus, a 1-eV junction as a bottom cell is one of the most remarkable methods to enhance efficiency of the triple-junction solar cells. [3-5] Therefore，the structures of InGaP/GaAs/InGaNAs/Ge [6] and InGaP/GaAs/$In_{0.3}Ga_{0.7}As$/Ge [5, 7] have been proposed and fabricated for high-efficiency tandem solar cells, both of which share a 1.0 eV sub-cell. However, the dilute nitride alloy InGaNAs (E_g=1.0 eV) is not practical to fabricate the GaAs-based multi-junction solar cells due to its very short lifetime of the minority carriers, although it has a satisfactory lattice matching with GaAs. [8-10] Another alternative is to adopt $In_{0.3}Ga_{0.7}As$ (E_g=1.0 eV) instead of InGaNAs as the sub-cell to achieve photocurrent match. [5] However, $In_{0.3}Ga_{0.7}As$ has a large lattice mismatch of 2.3 % with GaAs. [11] If $In_{0.3}Ga_{0.7}As$ film is directly grown on GaAs, a great number of defects will be introduced into the as-grown $In_{0.3}Ga_{0.7}As$ film due to the large lattice mismatch between them. Finally, the device performance will be significantly deteriorated due to the $In_{0.3}Ga_{0.7}As$ film of poor crystallinity.

It is well known that the insertion of a thin buffer layer between the substrate and the lattice-mismatched epilayer can effectively improve crystal quality of the epitaxial layers. [12-14] Recently, we have demonstrated the high-quality $In_{0.3}Ga_{0.7}As$ epitaxial layers on a 2-nm amorphous $In_{0.6}Ga_{0.4}As$ buffer layer on GaAs substrate by means of low temperature molecular beam epitaxy (LT-MBE). [15] An amorphous $In_{0.6}Ga_{0.4}As$ insert layer can be utilized as an elastic layer between $In_{0.3}Ga_{0.7}As$ epilayer and GaAs substrate. However, thickness of the $In_{0.6}Ga_{0.4}As$ is very sensitive for the crystallinity of the $In_{0.3}Ga_{0.7}As$ epilayer. In this work, effect of the $In_{0.6}Ga_{0.4}As$ thickness on the epitaxial growth of $In_{0.3}Ga_{0.7}As$ has been systematically investigated. We have experimentally demonstrated that epitaxial growth of strain-free $In_{0.3}Ga_{0.7}As$ layer on the GaAs substrate has been achieved using a 2-nm amorphous $In_{0.6}Ga_{0.4}As$ buffer layer. This work indicated that growing high-quality $In_{0.3}Ga_{0.7}As$ film on the GaAs substrate by inserting an amorphous $In_{0.6}Ga_{0.4}As$ buffer layer with appropriate thickness is a simple but effective approach.

2. Experimental details

The $In_{0.3}Ga_{0.7}As$ films were grown on the semi-insulated GaAs (001) substrates by MBE. High purity In (7N), Ga (7N) and As (7N) were used as the deposition sources, respectively. The GaAs substrates were primarily ultrasonically cleaned in chemicals and deionized water to remove the surface contaminations and finally dried by nitrogen gas before being put into the MBE load-lock chamber with a pressure of 3.2×10^{-8} Torr. The substrates were then transferred into the high vacuum MBE growth chamber under a pressure of 4.0×10^{-10} Torr and annealed at 600 °C for 15 min under As molecular beam protection to further remove the surface oxidized layer. The beam flux detectors attached to the MBE system were deployed to measure the flow rates of the deposition sources.[16] Before the growth of the $In_{0.3}Ga_{0.7}As$ layer, a $In_{0.6}Ga_{0.4}As$ buffer layer was firstly grown at the substrate temperature of 380 °C with a growth

rate of 0.05 nm/s. 4, 2, 1 and 0 nm thick $In_{0.6}Ga_{0.4}As$ buffer layers were then grown on this temperature, respectively. Finally, the substrate temperature was increased to 540 °C and a 500 nm-thick $In_{0.3}Ga_{0.7}As$ layer was deposited using a growth rate of 0.03 nm/s. The specialized electrochemical measurement systems called electrochemical quartz crystal microbalances (EQCMs) were utilized to monitor the thickness of as-grown films during the MBE growth.[17]

The crystalline quality of the as-grown films was characterized by high-resolution X-ray diffraction (HRXRD) using a Bruker D8 Discover with a Cu $K\alpha_1$ as the x-ray source. Cross-sectional high-resolution transmission electron microscopy (HRTEM) measurement was carried out to study the microstructure of the samples. The HRTEM samples were put into a JEOL 3000F field emission gun TEM (Tokyo, Japan) working at a voltage of 300kV, which gives a point to point resolution of 0.17 nm.

3. Results and discussions

In our previous study, we have found that the as-grown $In_{0.3}Ga_{0.7}As$ film is polycrystalline if the low-temperature amorphous $In_{0.6}Ga_{0.4}As$ buffer layer is thicker than 8 nm.[15] And the transformation of as-grown $In_{0.3}Ga_{0.7}As$ film from polycrystalline form to single-crystalline form occurs when the thickness of $In_{0.6}Ga_{0.4}As$ buffer layer is decreased to 4 nm. Figure 1(a) is the typical XRD 2θ-ω profile of the as-grown $In_{0.3}Ga_{0.7}As$ films grown on 4-nm- and 2-nm-thick amorphous $In_{0.6}Ga_{0.4}As$ buffer layer. Besides the diffraction peaks from the GaAs substrate, only the diffraction peaks corresponding to the $In_{0.3}Ga_{0.7}As$ (002) and (004) planes could be observed in the XRD patterns, confirming single crystallinity of the $In_{0.3}Ga_{0.7}As$ epilayer. We can clearly distinguish the $In_{0.3}Ga_{0.7}As$ (002) and GaAs (002) diffraction peaks from the Figure 1(a) inset. The crystalline quality of as-grown $In_{0.3}Ga_{0.7}As$ thin films is studied by XRD rocking curves, as shown in Figure 1(b). When thickness of the $In_{0.6}Ga_{0.4}As$ buffer layer is 4 nm, the full width at half maximum (FWHM) of XRD rocking curve is 980 arcsec, as shown in the Figure 1(b). The FWHM of as-grown $In_{0.3}Ga_{0.7}As$ film is 108 arcsec with thickness of the $In_{0.6}Ga_{0.4}As$ buffer layer reduced to 2 nm. The decrease in FWHM of the as-grown $In_{0.3}Ga_{0.7}As$ film grown on 2-nm-thick $In_{0.6}Ga_{0.4}As$ buffer layer indicates that the thin amorphous $In_{0.6}Ga_{0.4}As$ buffer layer can effectively reduce the lattice mismatch between the $In_{0.3}Ga_{0.7}As$ epilayer and the GaAs substrate. However, a further reduction in the thickness of the amorphous $In_{0.6}Ga_{0.4}As$ buffer will deteriorate the as-grown $In_{0.3}Ga_{0.7}As$ film quality, on the contrary. $In_{0.3}Ga_{0.7}As$ film grown on GaAs substrate with 1- and 0-nm-thick amorphous $In_{0.6}Ga_{0.4}As$ buffer layer ends up with the FWHM of 556 and 1292.9 arcsec, respectively. Evidently, too thin amorphous $In_{0.6}Ga_{0.4}As$ buffer layer can not efficiently release the misfit strain and trap the dislocations.

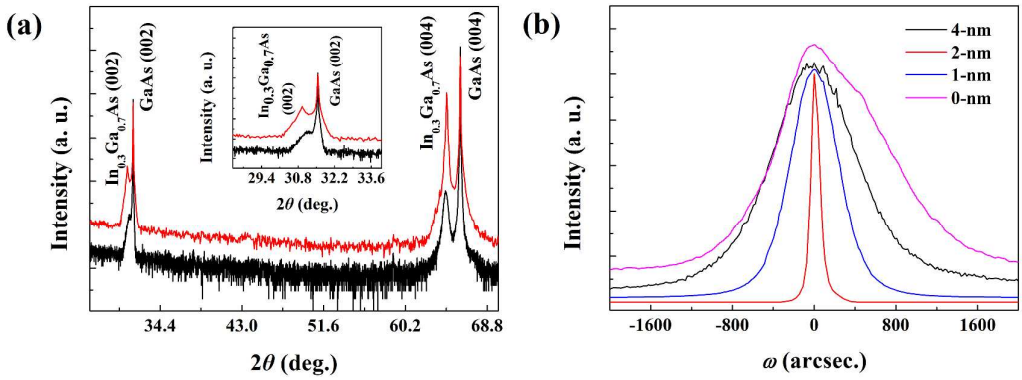

Figure 1(a) The typical XRD 2θ-ω profile of the as-grown $In_{0.3}Ga_{0.7}As$ films grown on 4-nm- (black line) and 2-nm- (red line) thick amorphous $In_{0.6}Ga_{0.4}As$ buffer layer, and the inset is the magnified view of the $In_{0.3}Ga_{0.7}As$ (002) and GaAs (002) diffraction peaks, (b) XRD rocking curves of the as-grown $In_{0.3}Ga_{0.7}As$ (004) with different thickness amorphous $In_{0.6}Ga_{0.4}As$ buffer layer.

In order to study the strain state in as-grown $In_{0.3}Ga_{0.7}As$ films, the RSM measurements are carried out around the $In_{0.3}Ga_{0.7}As$/GaAs (224) reciprocal lattice point, as shown in Figure 2. The vertical and horizontal axes represent the reciprocal lattice of the [110] (Q_x) and [001] (Q_z) directions, respectively. The GaAs substrate and the $In_{0.3}Ga_{0.7}As$ epilayer diffraction patterns are well resolved in Figure 2, and for the as-grown $In_{0.3}Ga_{0.7}As$ film with 4-nm-thick $In_{0.6}Ga_{0.4}As$ buffer layer, the $In_{0.3}Ga_{0.7}As$ epilayer diffraction peak broadening occurs along both the mosaic direction and the lateral direction, [18] as shown in Figure 2(a). It has been reported that the epilayer diffraction peak broadening is caused by different crystal imperfections. Firstly, the epilayer diffraction peak broadening along the mosaic direction means that it is presence of mosaic block, which slightly rotate the allowable diffraction planes in their vicinity. [19, 20] Secondly, the diffraction peak broadening along the [110] direction indicates that lateral correlation length is limited, which can be related to an average crystallite size that exhibits coherent diffraction.[21, 22] The diffraction peak broadening of the as-grown $In_{0.3}Ga_{0.7}As$ film grown on 4-nm-thick $In_{0.6}Ga_{0.4}As$ buffer layer indicates that the 4-nm amorphous $In_{0.6}Ga_{0.4}As$ buffer layer cannot effectively reduces the lattice mismatch between the $In_{0.3}Ga_{0.7}As$ epilayer and the GaAs substrate.

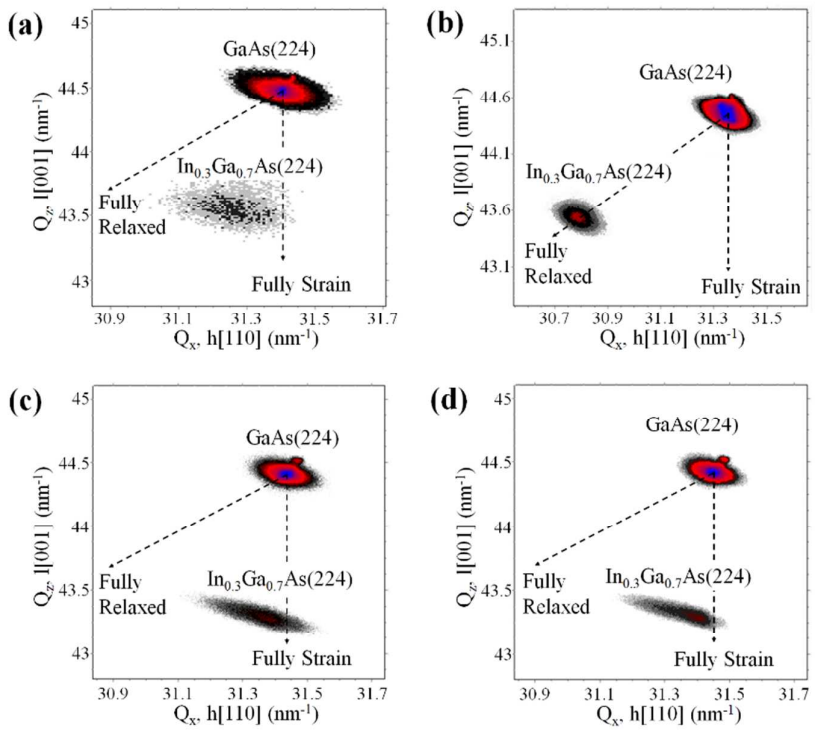

Figure 2 Reciprocal space mappings with (224) reflection of the $In_{0.3}Ga_{0.7}As$ epilayers with (a) 4-nm-, (b) 2-nm-, (c) 1-nm- and 0-nm-thick $In_{0.6}Ga_{0.4}As$ buffer layer. The up diffraction pattern is GaAs substrate, the down diffraction pattern is $In_{0.3}Ga_{0.7}As$ epilayer.

Figure 2(b) shows the asymmetric (224) RSM of the as-grown $In_{0.3}Ga_{0.7}As$ film with 2-nm-thick $In_{0.6}Ga_{0.4}As$ buffer layer. We can clearly observe that the diffraction pattern of $In_{0.3}Ga_{0.7}As$ (224) display an approximately circle shape, which manifests an improved crystalline quality of the $In_{0.3}Ga_{0.7}As$ film. [23] The asymmetric (224) RSMs of the as-grown $In_{0.3}Ga_{0.7}As$ films with 1-nm and 0-nm-thick $In_{0.6}Ga_{0.4}As$ buffer layer are show in Figures 2(c) and (d), respectively. From Figures 2(c) and (d), on the contrary, a strong mosaic structure can be observed in the $In_{0.3}Ga_{0.7}As$ films through a large extension diffraction pattern in the [110] direction. It indicates that the too thin thickness of amorphous $In_{0.6}Ga_{0.4}As$ buffer layer will deteriorate the as-grown $In_{0.3}Ga_{0.7}As$ film quality.

The lattice parameters of as-grown $In_{0.3}Ga_{0.7}As$ layers can be calculated from the $In_{0.3}Ga_{0.7}As$ (224) RSMs. The lattice parameters in the in-plane ($a_{//}$) and the perpendicular ($a_{\perp}$) directions of $In_{0.3}Ga_{0.7}As$ layers can be therefore obtained from the following equations: [24]

$$Q_x = \frac{2\pi}{a_{//}}\sqrt{h^2+k^2} = \frac{4\pi}{\lambda}\sin\theta\sin(\omega-\theta), \quad (1)$$

$$Q_z = \frac{2\pi}{a_{\perp}}l = \frac{4\pi}{\lambda}\sin\theta\cos(\omega-\theta), \quad (2)$$

where λ is the wavelength of x-rays. Additionally, the epilayer strain with respect to completely relaxed material is defined as

$$\varepsilon_{\perp,//} = \frac{a_{\perp,//} - a_s}{a_s}, \quad (3)$$

where $\varepsilon_{\parallel}$ and $\varepsilon_{\perp}$ denote the in-plane and perpendicular strain, respectively; a_s is the lattice parameter of substrate. The fully relaxed $In_{0.3}Ga_{0.7}As$ lattice parameter of 5.7749 Å can be calculated from a linear interpolation (Vegard's law) between the lattice constants of the binary alloy constituents (GaAs and InAs). [25] Thus, lattice parameters and the strain values of the as-grown $In_{0.3}Ga_{0.7}As$ layers are shown in Table 1.

Table 1 The lattice constants of the as-grown $In_{0.3}Ga_{0.7}As$ layers with different thickness of the amorphous $In_{0.6}Ga_{0.4}As$ buffer layer.

Buffer layer thickness (nm)	Lattice parameters (Å)		Strain values (%)		In-plane relaxation rates (%)
	$a_{\parallel}$	$a_{\perp}$	$\varepsilon_{\parallel}$	$\varepsilon_{\perp}$	
4	5.6816	5.7688	-1.62	-0.11	23.20
2	5.7708	5.7747	-0.07	-0.003	96.63
1	5.6614	5.8044	-1.97	0.51	6.60
0	5.6567	5.8020	-2.05	0.47	2.74

From Table 1, we can observe that the epilayer endures different strain for different thickness of the amorphous $In_{0.6}Ga_{0.4}As$ buffer layer. The $In_{0.3}Ga_{0.7}As$ layer grown on 4-nm-thick buffer is compressively strained in both in-plane and perpendicular directions. When the thickness of amorphous $In_{0.6}Ga_{0.4}As$ layer is 2-nm-thick, the as-grown $In_{0.3}Ga_{0.7}As$ layer is nearly strain-free. It means that the compressive strain endured by the as-grown $In_{0.3}Ga_{0.7}As$ layer is getting less with decreasing the thickness of amorphous $In_{0.6}Ga_{0.4}As$ layer. However, when the buffer layer thickness decreases to 1-nm or less, the as-grown $In_{0.3}Ga_{0.7}As$ layers are still compressively strained in the in-plane direction. In particular, the as-grown $In_{0.3}Ga_{0.7}As$ layers under tensile strain in the perpendicular direction due to too thin buffer layer. The results indicate that the strain state of as-grown $In_{0.3}Ga_{0.7}As$ films is strongly affected by the thickness of the amorphous $In_{0.6}Ga_{0.4}As$ buffer layer.

The strain relaxation of as-grown $In_{0.3}Ga_{0.7}As$ films can be defined by: [23]

$$R = \frac{a_{//} - a_s}{a_{relaxed} - a_s}. \quad (4)$$

The relaxation degrees are shown in Table 1. According to the relaxation degree, the RSMs diffraction pattern of the epilayers may have different positions, there are a fully relaxed, a partially relaxed, or a fully strained layer. [22, 26] Depending to relaxation degree, we can confirm that the as-grown $In_{0.3}Ga_{0.7}As$ film with 4-nm-thick $In_{0.6}Ga_{0.4}As$ buffer layer is a partially relaxed layer, the $In_{0.3}Ga_{0.7}As$ film with

2-nm-thick $In_{0.6}Ga_{0.4}As$ buffer layer is an approximately fully relaxed layer, and the $In_{0.3}Ga_{0.7}As$ film with 1- and 0-nm-thick $In_{0.6}Ga_{0.4}As$ buffer layer are approximately fully strained layers. The results indicate that the 2-nm-thick amorphous $In_{0.6}Ga_{0.4}As$ buffer layer can effectively reduce the mismatch-strain between the $In_{0.3}Ga_{0.7}As$ epilayer and GaAs substrate, obtained fully relaxed and high-quality $In_{0.3}Ga_{0.7}As$ film.

Cross-sectional TEM investigation is carried out to understand the heterostructure of $In_{0.3}Ga_{0.7}As$ films grown on GaAs substrates. Figures 3(a) and (b) are the typical cross-sectional HRTEM images of $In_{0.3}Ga_{0.7}As$ film grown on GaAs substrate with 4-nm and 2-nm-thick $In_{0.6}Ga_{0.4}As$ buffer layer, respectively. Figure 3(a) shows that the as-grown $In_{0.3}Ga_{0.7}As$ film with 4-nm-thick amorphous $In_{0.6}Ga_{0.4}As$ buffer layer is single-crystalline, in spite of a relatively large density of dislocations existing in the film. We can observe that the $In_{0.3}Ga_{0.7}As$ epitaxial film is of a high degree of structural perfection, when the amorphous $In_{0.6}Ga_{0.4}As$ buffer layer thickness is 2 nm, as shown in Figure 3(b). This result is consistent with the XRD result.

From Figures 3(a) and (b), it can be easily notice that the alignment of atoms in as-grown $In_{0.6}Ga_{0.4}As$ buffer layer are completely disordered, or in the other term, amorphous. A high density of dislocations are nucleated in the $In_{0.6}Ga_{0.4}As/In_{0.3}Ga_{0.7}As$ interface, and extended to the $In_{0.3}Ga_{0.7}As$ epilayer, Figure 3(a). Conversely, most of defects 'drown' in the amorphous $In_{0.6}Ga_{0.4}As$ buffer layer near the interface. As the epilayer thickness gradually increase, the threading dislocations cannot be observed within the $In_{0.3}Ga_{0.7}As$ epitaxial film, as shown in Figure 3(b). We observe that the $In_{0.6}Ga_{0.4}As$ buffer layer of the $In_{0.3}Ga_{0.7}As/2\text{-nm-}In_{0.6}Ga_{0.4}As/GaAs$ structure is an amorphous state, which has been verified by its halo selected area electron diffraction (SAED) pattern, as seen in Figure 3(c).

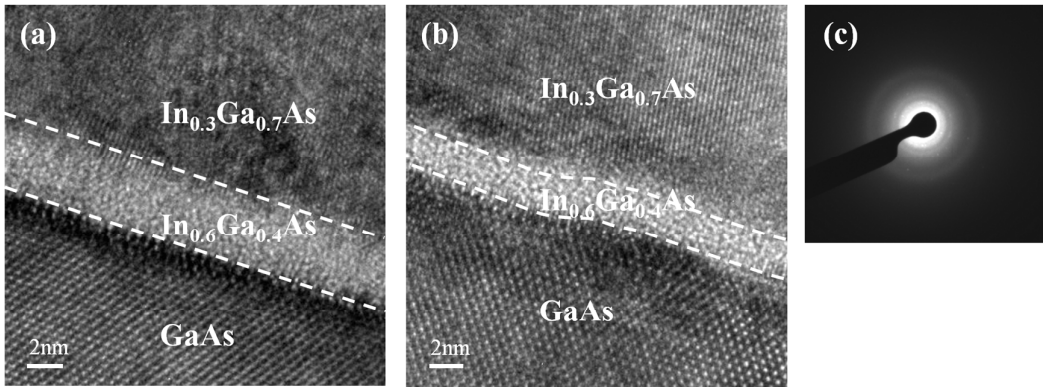

Figure 3 Cross-sectional HRTEM images of the $In_{0.3}Ga_{0.7}As$/4-nm (a), 2-nm-thick (b) $In_{0.6}Ga_{0.4}As$/GaAs heterostructure, respectively. (c) the SAED pattern from the $In_{0.6}Ga_{0.4}As$ buffer layer of the $In_{0.3}Ga_{0.7}As/2\text{-nm-}In_{0.6}Ga_{0.4}As/GaAs$ heterostructure.

When the amorphous $In_{0.6}Ga_{0.4}As$ buffer layer is 4-nm thick, it can not well release the misfit strain between the $In_{0.3}Ga_{0.7}As$ epilayer and the substrate, as discovered by RSM, leading to a poor quality $In_{0.3}Ga_{0.7}As$ film. When the optimal thickness of the amorphous $In_{0.6}Ga_{0.4}As$ buffer layer is achieved, the 2-nm-thick

amorphous $In_{0.6}Ga_{0.4}As$ buffer will not only efficiently release the misfit strain between the $In_{0.3}Ga_{0.7}As$ epilayer and the substrate, and trap the threading and misfit dislocations, but also keep the function as a substrate for heteroepitaxial growth of $In_{0.3}Ga_{0.7}As$ film. Conversely, to further reducing the amorphous $In_{0.6}Ga_{0.4}As$ buffer layer thickness will deteriorate the crystal quality of as-grown $In_{0.3}Ga_{0.7}As$ film. The as-grown $In_{0.3}Ga_{0.7}As$ films FWHM values are 556 and 1292.9 arcsec from its XRD rocking curves with 1- and 0-nm-thick amorphous $In_{0.6}Ga_{0.4}As$ buffer layer, respectively. According to the previous description, the crystal quality of as-grown $In_{0.3}Ga_{0.7}As$ films is strongly affected by the thickness of the low-temperature large-mismatched amorphous $In_{0.6}Ga_{0.4}As$ buffer layer. An appropriate thickness for the amorphous $In_{0.6}Ga_{0.4}As$ buffer layer is preferable to accomplish its effect, to obtain the high quality and fully relaxed $In_{0.3}Ga_{0.7}As$ films when amorphous $In_{0.6}Ga_{0.4}As$ buffer layer thickness is 2-nm.

We have then tried to understand how the amorphous $In_{0.6}Ga_{0.4}As$ buffer layer is formed in this work. Firstly, the lattice mismatch between $In_{0.6}Ga_{0.4}As$ and GaAs is as large as 4.3% that will result in large misfit strain between them. When $In_{0.6}Ga_{0.4}As$ materials are grown on GaAs substrates, shrink in chemical bond length for both In-As and Ga-As can be clearly observed, and higher In component corresponds to more shrinkage.[11, 27] Severe lattice distortion is consequently generated at the $In_{0.6}Ga_{0.4}A$/GaAs interface, particularly, the In component is as high as 0.6. Secondly, In has a larger atomic radius and average mass than Ga and As. It means that In atoms migrate slower on the substrate surfaces. Especially, in this work, the growth of $In_{0.6}Ga_{0.4}As$ buffer layer with high In component is adopted for a relatively low growth temperature, which would result in a large proportion of In atoms cannot obtain enough kinetic energy to migrate on GaAs surface freely. These In atoms with larger atomic radii dwell randomly on the substrate surfaces that effectively hamper the migration of Ga and As atoms, and therefore the nucleation of $In_{0.6}Ga_{0.4}As$. In this regards, the amorphous $In_{0.6}Ga_{0.4}As$ is formed on GaAs substrate at the low growth temperature.

The previous studies have pointed out that the low-temperature buffer layer will provide low-energy sites for the dislocations nucleation and point defects, which on the one hand effectively reduces the threading dislocation density in heteroepitaxy, and on the other hand releases the misfit strain between the substrate and epilayer. [28] Rahman *et al.* [29] have carried out a similar experiment to grow $Si_{0.75}Ge_{0.25}$ film on Si substrate using a low-temperature ultrathin amorphous buffer layer. They find that the ultrathin amorphous buffer layer have a great effect on the strain relaxation during the heteroepitaxial growth. The amorphous buffer layer will act as the 'free-standing' compliant layer to accommodate the misfit strain in the epilayer, and moreover, as trapping sites for threading dislocations. The previous studies have well explained that the effects of low-temperature ultrathin amorphous buffer layers on the strain relaxation in the heteroepitaxal film. According to those pioneers' studies, the ultrathin amorphous $In_{0.6}Ga_{0.4}As$ layer in this work will trap threading dislocations and release the misfit strain. What's more, although a very high density of point defects and dislocations are generated within the ultrathin amorphous $In_{0.6}Ga_{0.4}As$

buffer layer, the defects are confined in the low-temperature buffer layer, without extending to the subsequently grown $In_{0.3}Ga_{0.7}As$ epilayer. In such a way, the defect density of as-grown $In_{0.3}Ga_{0.7}As$ epilayer is highly diminished.

4. Conclusions

Large-mismatched amorphous $In_{0.6}Ga_{0.4}As$ layers have been growth on GaAs substrates using low-temperature growth by MBE, and acted as buffer layer for the subsequent epitaxial growth of $In_{0.3}Ga_{0.7}As$ films. For $In_{0.3}Ga_{0.7}As$ layer grown on the top of the 4, 2, 1 and 0-nm-thick amorphous $In_{0.6}Ga_{0.4}As$ buffer layer, its FWHM of $In_{0.3}Ga_{0.7}As$ XRD rocking curve is 980, 108, 556 and 1292.9 arcsec, respectively. Given an appropriate thickness of 2 nm, this amorphous $In_{0.6}Ga_{0.4}As$ buffer layer can efficiently releases the misfit strain between the $In_{0.3}Ga_{0.7}As$ epilayer and the GaAs substrate, trap the threading and misfit dislocations from propagating to the following $In_{0.3}Ga_{0.7}As$ epilayer, leading to a high-crystallinity $In_{0.3}Ga_{0.7}As$ film. The RSM results reveal that as-grown $In_{0.3}Ga_{0.7}As$ film with low dislocation density and good strain relaxation has been achieved by using an amorphous buffer layer of 2 nm. In other words, 2 nm $In_{0.6}Ga_{0.4}As$/GaAs heterostructure provides an outstanding "virtual substrate" for epitaxial growth of high-quality $In_{0.3}Ga_{0.7}As$ film. This work demonstrates a much simpler approach to achieve high-quality $In_{0.3}Ga_{0.7}As$ film on GaAs substrate, and therefore is of huge potential for the InGaAs-based high-efficiency photovoltaic industry.

Acknowledgements

The authors gratefully acknowledge financial support from the National Science Fund for Excellent Young Scholars of China (No. 51422203), National Science Foundation of China (No. 51372001), National Key Basic Research Project of China (973 Project), Excellent Youth Foundation of Guangdong Scientific Committee (No. S2013050013882), Key Project in Science and Technology of Guangdong Province (No. 2011A080801018), and the Fundamental Research Funds for the Central Universities (x2c1-D2142w).

References

1. D. Shahrjerdi, S. W. Bedell, C. Ebert, C. Bayram, B. Hekmatshoar, K. Fogel, P. Lauro, M. Gaynes, T. Gokmen, J. A. Ott and D. K. Sadana, *Appl. Phys. Lett.*, 2012, **100**(5), 053901-3.
2. W. Guter, J. Schone, S. P. Philipps, M. Steiner, G. Siefer, A. Wekkeli, E. Welser, E. Oliva, A. W. Bett and F. Dimroth, *Appl. Phys. Lett.*, 2009, **94**(22), 223504-3.
3. S. R. Kurtz, D. Myers and J. M. Olson, *Photovoltaic Specialists Conference, 1997. Conference Record of the Twenty-Sixth IEEE*, 1997, pp. 875–878.
4. D. J. Friedman, J. F. Geisz, A. G. Norman, M. W. Wanlass and S. R. Kurtz, *Photovoltaic Energy Conversion, Conference Record of the 2006 IEEE 4th World Conference on*, 2006, pp. 598-602.
5. J. F. Geisz, S. Kurtz, M. W. Wanlass, J. S. Ward, A. Duda, D. J. Friedman, J. M. Olson, W. E. McMahon, T. E. Moriarty and J. T. Kiehl, *Appl. Phys. Lett.*, 2007,

91(2), 023502-3.
6. R. R. King, D. Bhusari, D. Larrabee, X. Q. Liu, E. Rehder, K. Edmondson, H. Cotal, R. K. Jones, J. H. Ermer, C. M. Fetzer, D. C. Law and N. H. Karam, *Prog. Photovoltaics*, 2012, **20**(6), 801-815.
7. D. C. Law, R. R. King, H. Yoon, M. J. Archer, A. Boca, C. M. Fetzer, S. Mesropian, T. Isshiki, M. Haddad, K. M. Edmondson, D. Bhusari, J. Yen, R. A. Sherif, H. A. Atwater and N. H. Karam, *Sol. Energy Mater. Sol. Cells.*, 2010, **94**(8), 1314-1318.
8. T. W. Kim, T. J. Garrod, K. Kim, J. J. Lee, S. D. LaLumondiere, Y. Sin, W. T. Lotshaw, S. C. Moss, T. F. Kuech, R. Tatavarti and L. J. Mawst, *Appl. Phys. Lett.*, 2012, **100**(12), 121120-4.
9. R. Trotta, A. Polimeni and M. Capizzi, *Adv. Funct. Mater.*, 2012, **22**(9), 1782-1801.
10. Y. Ohshita, H. Suzuki, N. Kojima, T. Tanaka, T. Honda, M. Inagaki and M. Yamaguchi, *J. Cryst. Growth*, 2011, **318**(1), 328-331.
11. T. L. Lee, M. R. Pillai, J. C. Woicik, G. Labanda, P. F. Lyman, S. A. Barnett and M. J. Bedzyk, *Phys. Rev. B: Condens. Matter Mater. Phys.*, 1999, **60**(19), 13612-13618.
12. K. Zhang, S. J. Kim, Y. Zhang, T. Heeg, D. G. Schlom, W. Shen and X. Pan, *J. Phys. D: Appl. Phys.*, 2014, **47**(10), 105302-105306.
13. M. Kawano, S. Yamada, K. Tanikawa, K. Sawano, M. Miyao and K. Hamaya, *Appl. Phys. Lett.*, 2013, **102**(12), 121908-3.
14. T. Y. Wang, S. L. Ou, R. H. Horng and D. S. Wuu, *CrystEngComm*, 2014, **16**(25), 5724-5731.
15. F. L. Gao and G. Q. Li, *Appl. Phys. Lett.*, 2014, **104**(4), 042104-5.
16. J. R. Arthur, *Surf. Sci.*, 2002, **500**(1-3), 189-217.
17. X. Du, Y. Du and S. M. George, *J. Vac. Sci. Technol. A*, 2005, **23**(4), 581-588.
18. J. M. Chauveau, Y. Androussi, A. Lefebvre, J. Di Persio and Y. Cordier, *J. Appl. Phys.*, 2003, **93**(7), 4219-4225.
19. H. Lin, Y. J. Huo, Y. W. Rong, R. Chen, T. I. Kamins and J. S. Harris, *J. Cryst. Growth*, 2011, **323**(1), 17-20.
20. M. W. Dashiell, H. Ehsani, P. C. Sander, F. D. Newman, C. A. Wang, Z. A. Shellenbarger, D. Donetski, N. Gu and S. Anikeev, *Sol. Energy Mater. Sol. Cells.*, 2008, **92**(9), 1003-1010.
21. C. H. Jang, M. R. Sardela, S. H. Kim, Y. J. Song and N. E. Lee, *Appl. Surf. Sci.*, 2006, **252**(15), 5326-5330.
22. M. Erdtmann and T. A. Langdo, *J. Mater. Sci.: Mater. Electron*, 2006, **17**(2), 137-147.
23. M. C. Tseng, R. H. Horng, D. S. Wuu and M. D. Yang, *IEEE. J. Quantum. Elect.*, 2011, **47**(11), 1434-1442.
24. A. R. Khan, K. Mundboth, J. Stangl, G. Bauer, H. von Kanel, A. Fedorov, G. Isella and D. Colombo, *Emerging Technologies, 2005. Proceedings of the IEEE Symposium on*, 2005, pp. 323-328.
25. M. Fatemi and R. E. Stahlbush, *Appl. Phys. Lett.*, 1991, **58**(8), 825-827.

26. T. Roesener, V. Klinger, C. Weuffen, D. Lackner and F. Dimroth, *J. Cryst. Growth*, 2013, **368**, 21-28.
27. J. C. Woicik, *Phys. Rev. B: Condens. Matter Mater. Phys.*, 1998, **57**(11), 6266-6269.
28. Y. H. Luo, J. Wan, R. L. Forrest, J. L. Liu, G. Jin, M. S. Goorsky and K. L. Wang, *Appl. Phys. Lett.*, 2001, **78**(4), 454-456.
29. M. M. Rahman, S. Q. Zheng, M. Mori, T. Tambo and C. Tatsuyama, *J. Appl. Phys.*, 2006, **100**(5), 053505-5.